ELSEVIER

Biochimica et Biophysica Acta 1567 (2002) 6–12

BIOCHIMICA ET BIOPHYSICA ACTA
BBA

www.bba-direct.com

The interaction of α-tocopherol with bilayers of 1-palmitoyl-2-oleoyl-phosphatidylcholine

Xiaoyuan Wang[1], Peter J. Quinn*

Division of Life Sciences, King's College London, 150 Stamford Street, London SE1 9NN, United Kingdom

Received 3 May 2002; received in revised form 2 October 2002; accepted 16 October 2002

Abstract

The effect of α-tocopherol on the structure and phase behaviour of 1-palmitoyl-2-oleoyl-phosphatidylcholine was examined by real-time synchrotron X-ray diffraction and freeze-fracture electron microscopic methods. X-ray scattering intensity was recorded from mixed aqueous dispersions of phospholipid with 2.5, 5, 10 and 20 mol% α-tocopherol during temperature scans at 3 °/min between −25 and 10 °C. A ripple structure is induced by the presence of α-tocopherol that coexists with the ripple phase characteristic of the pure phospholipid in mixtures containing 2.5 mol% α-tocopherol but completely replaces it in mixtures containing greater proportions of α-tocopherol. Freeze-fracture replicas of dispersions containing 5 mol% α-tocopherol indicate a ripple phase with a periodicity of about 9 nm. Increasing amounts of α-tocopherol result in a progressive reduction in temperature of the gel to liquid–crystal phase transition and broadening of the transition. Two lamellar phases coexist in the liquid–crystal state, one with a spacing of 6.4 nm assigned to an α-tocopherol-enriched lamellar structure and the other with a lamellar repeat of 6.1 nm corresponding to bilayers of pure phospholipid.

Keywords: α-Tocopherol; Phospholipid bilayer; X-ray diffraction; Phosphatidylcholine; Vitamin E; Ripple phase

1. Introduction

α-Tocopherol is believed to have two primary functions in cells. Its major role is regarded to be to act as an antioxidant to prevent free radical damage to tissues and specifically to unsaturated lipids of membranes [1–5]. The second function is to stabilize the structure of membranes by forming complexes with lipid hydrolytic products such as lysophosphatides and free fatty acids [6]. A number of studies [7–13] have attempted to probe the location and function of α-tocopherol in membranes by determining its molecular interaction with phospholipids. These studies concluded that α-tocopherol has its hydroxyl group located near the polar interface of the lipid bilayer with the prenyl side chain extending into the hydrocarbon interior. Intercalation of the molecule between the phospholipids affects the thermotropic phase behaviour of the phospholipid such that increasing proportions of α-tocopherol progressively broaden the temperature range of the gel to liquid–crystalline phase transition of phosphatidylcholines. It has been consistently observed in the thermal studies of mixtures of α-tocopherol with saturated phosphatidylcholines that the presence of α-tocopherol apparently eliminates the pretransition enthalpy [8,14–18]. Furthermore, evidence from synchrotron X-ray diffraction and freeze-fracture electron microscopy have shown that different ripple structures are induced by α-tocopherol and which extend to temperatures well below the main transition of the pure phospholipids [19].

The effect of α-tocopherol on phospholipid structure and phase behaviour differs depending on the headgroup, the length and extent of unsaturation of the carbon chains of the phospholipids [19–23]. In biological membranes, most phospholipids possess mixed acyl chain composition including fatty acyl residues with one or more *cis* double bonds [24]. To more closely mimic the lipid matrix of biological membranes, bilayer dispersions of 1-palmitoyl-2-oleoyl-

Abbreviations: POPC, 1-palmitoyl-2-oleoyl-*sn*-phosphatidylcholine; SAXS, small-angle X-ray scattering (2θ=0.043–7.9°); WAXS, wide-angle X-ray scattering (2θ=8–60°); L_α, lamellar liquid–crystalline phase; L_β, lamellar gel phase; P_β, ripple phase

* Corresponding author. Tel./fax: +44-207-8484408.

E-mail address: p.quinn@kcl.ac.uk (P.J. Quinn).

[1] Present address: Department of Biochemistry and Molecular Biology, Medical School, University of Texas-Houston, Houston, TX 77225, USA.

0005-2736/02/$ - see front matter © 2002 Elsevier Science B.V. All rights reserved.
PII: S0005-2736(02)00636-3

phosphatidylcholine were used to examine the effects of the presence of α-tocopherol. The use of synchrotron X-ray diffraction methods has allowed us to characterise the phase behaviour of mixed aqueous dispersions of the phospholipid with α-tocopherol as well as identify an induced ripple phase. Of particular relevance to biological membranes is the finding that phase separated domains of phospholipid enriched in α-tocopherol coexist with pure phospholipid bilayers in the fluid phase.

2. Materials and methods

1-Palmitoyl-2-oleoyl-*sn*-phosphatidylcholine (POPC) was purchased from Avanti Polar Lipids (Alabaster) and α-tocopherol from Acros Organics (Geel, Belgium). The lipids were dissolved in chloroform and mixed in appropriate proportions to achieve the desired molar fractions (mol% = 100% × mol α-tocopherol/(mol α-tocopherol + mol POPC)). The solvent was evaporated under a stream of oxygen-free dry nitrogen and stored for 24 h under vacuum to remove any remaining traces of solvent. The lipid mixtures were hydrated with an equal weight of water at 80 °C for at least 1 h and dispersed by a rotamixer until homogeneous dispersions were obtained. The lipid dispersions were stored at 4 °C for 24 h before examination. The method of preparation and storage gave reproducible phase behaviour when samples prepared at different times were examined by X-ray diffraction.

Synchrotron X-ray diffraction experiments were performed using a monochromatic (0.15405 nm) focused X-ray beam at station 8.2 of the Daresbury Synchrotron Radiation Laboratory, UK. The camera configuration allowed detection of small-angle and wide-angle X-ray scattering with a minimum of parallax error [25]. The beam line generates a flux of 4×10^{10} photons per second with a focal spot size of 0.3×3 mm^2 (V × H) when the synchrotron radiation source is operating at a nominal 200 mA. The samples were mounted in a slot (1 × 5 mm) cut in a 1-mm-thick copper plate sandwiched between a pair of thin mica sheets. The sandwich was clamped to the silver block containing the temperature sensing and modulating elements of a cryomicroscope stage (Linkam Scientific Instruments, UK). Temperature scans in heating and cooling modes were performed at 3°/min. X-ray scattering intensities at small angles ($2\theta = 0.043–7.9°$) were recorded using a multiwire quadrant detector. X-ray scattering intensities at wide angles ($2\theta = 8–60°$) were recorded using an INEL curved linear-wire detector (INstrumentation Electronique, France). Data were acquired in 400 consecutive time frames of 5 s and separated by a dead time between frames of 50 ms. Experimental data were analysed using the OTOKO software (EMBL, Hamburg, Germany) programme [26]. Scattering intensities at low-angles (SAXS) were corrected for fluctuations in beam intensity and detector response recorded from an ^{55}Fe source. Spatial calibrations were obtained using 21 orders of wet rat-tail collagen ($d = 67$ nm) [27]. The scattering intensities recorded at wide angles (WAXS) by the INEL detector were corrected for scattering from an empty cell and spatial calibrations were established from high-density polyethylene (0.4166, 0.3780, 0.3014 nm) [28]. The reciprocal spacing $S = 1/d = 2\sin(\theta)/\lambda$, where d, λ, θ are the repeat distance, X-ray wavelength and the diffraction angle, respectively.

Freeze-fracture electron microscopy: Samples and tools used for sample manipulation were equilibrated at the desired temperature for at least 15 min. For cryofixation, a small drop of the suspension was sandwiched between two copper plates and manually plunged into liquid propane. Fracturing and shadowing were performed at −150 °C in a BAF 400D freeze-etching device (Balzers, Liechtenstein). The replicas were cleaned with chloroform and examined using a CEM 902A (Zeiss, Germany) electron microscope.

3. Results and discussion

The effect of α-tocopherol on the phase behaviour of POPC was examined by synchrotron X-ray diffraction methods. Plots of X-ray diffraction intensity vs. scattering angle were recorded from aqueous dispersions of the pure phospholipid and codispersions of phospholipid with α-tocopherol during a heating scan from −25 to 10 °C at 3°/min. Data were collected simultaneously in the SAXS and WAXS regions, respectively. The result of a heating scan of a dispersion of the pure phospholipid is shown in Fig. 1. At temperatures less than −12 °C, a lamellar phase is observed with a *d*-spacing of 6.2 nm; there is a sharp symmetrical peak in the WAXS region centred at 0.43 nm indicating that the hydrocarbon chains are packed in a gel phase configuration and oriented close to perpendicular to the plane of the bilayer. Two sharp peaks centred at spacings of 0.39 and 0.37 nm represent reflections from hexagonal ice. Upon heating above −12 °C, there is a progressive expansion of lattice spacings for both SAXS and WAXS regions and appearance of a peak at about 16.5 nm. This is shown more clearly in a plot of the logarithm of scattering intensity presented in Fig. 1c and is assigned as a repeat spacing of a ripple phase (P_β). Evidence of a transition to an L_α phase first appears in the SAXS region as a shoulder on the first-order lamellar repeat of the P_β phase at about −2 °C and continues throughout the ice melting at 0 °C. The transition coincides with a decrease in intensity of the sharp WAXS peak at 0.43 nm (−5 °C) and its replacement by a broad scattering band at 0.45 nm (5 °C) (Fig. 1b) indicating disordering of the hydrocarbon chain packing associated with transition to the liquid–crystal phase. The mid-point of the gel to liquid–crystal phase transition is about 0.5 °C. This is a few degrees higher than recorded for phospholipid dispersed in aqueous media containing solutes that perturb the temperature of ice formation and values for the main

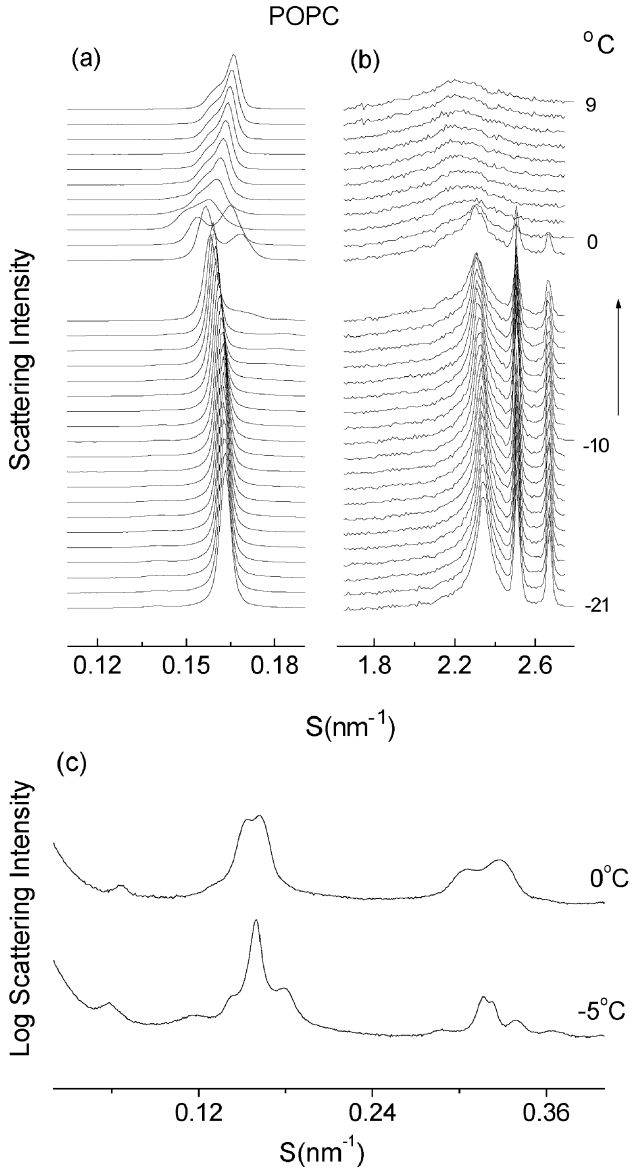

Fig. 1. Plots of SAXS (a) and WAXS (b) intensity profiles versus reciprocal spacing as a function of temperature of a fully hydrated dispersion of POPC recorded during a heating scan from −21 to 9 °C at 3°/min. Each diffraction pattern represents scattering accumulated in 10 s. (c) The profile in SAXS recorded at 0 and −5 °C are plotted as the logarithm of intensity to emphasize the minor bands.

transition around −2.3 °C are commonly reported [Lipidat data base].

The results of a heating scan of a mixed aqueous dispersion of POPC containing 2.5 mol% α-tocopherol are presented in Fig. 2. At temperatures below 0 °C, additional peaks are observed due to the presence of α-tocopherol. These peaks have *d*-spacings of 7.60, 5.56, 3.50, 3.21 and 2.95 nm in the SAXS region, which are shown more distinctly in the plot of the logarithm of scattering intensity recorded at −5 °C in Fig. 2c. The temperature dependence of the *d*-spacings of these additional peaks differ from that observed for the lamellar phase with a *d*-spacing of 6.20 nm and they are assigned to reflections from a ripple phase. A ripple phase characterised by a (1,0) reflection at 16.7 nm (−5 °C) was observed below the main transition (Fig. 2c); however, the scattering intensities of this ripple phase are reduced compared with the pure phospholipid and the temperature range is narrowed. Judging from the temperature dependence of the sharp WAXS peak from the hydrocarbon chain, packing the mid-point of the transition from gel to liquid–crystal phase is about −1.5 °C. Two lamellar phases coexist in the fluid phase; one corresponding to the

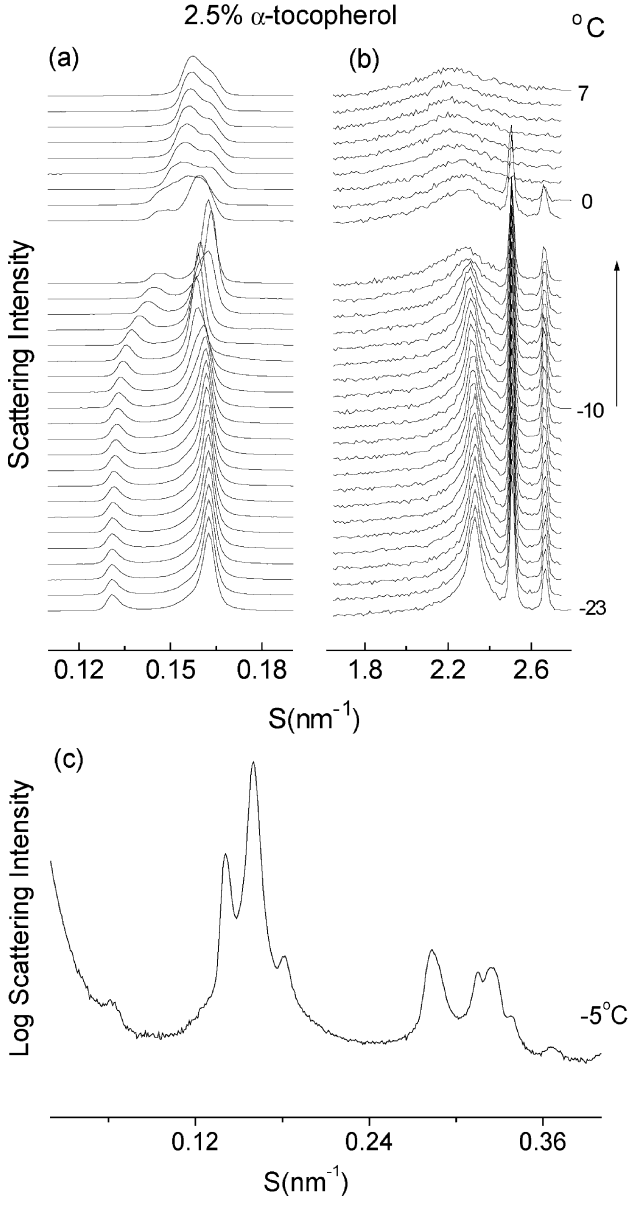

Fig. 2. Plots of SAXS (a) and WAXS (b) intensity profiles versus reciprocal spacing as a function of temperature of a codispersion of 2.5 mol% α-tocopherol in POPC recorded during a heating scan from −23 to 7 °C at 3°/min. Each diffraction pattern represents scattering accumulated in 10 s. (c) The profile in SAXS recorded at −5 °C is plotted at the logarithm of intensity to emphasize the minor bands.

lamellar phase of pure POPC (*d*-spacing 6.10 nm) and a more intense peak with a *d*-spacing of 6.36 nm assigned to an α-tocopherol enriched phase.

Further studies were performed on mixed dispersions of POPC containing greater proportions of α-tocopherol to confirm the trends observed with 2.5 mol% α-tocopherol. Fig. 3a,b shows X-ray diffraction patterns recorded during a heating scan at 3°/min of a mixed aqueous of dispersion of POPC containing 5 mol% α-tocopherol. The lamellar diffraction bands centred at 6.3 nm (−20 °C) were considerably broadened compared with the corresponding peaks present in the mixture containing only 2.5 mol% α-tocopherol (Fig. 2a). These broad bands can be resolved into two peaks with spacings corresponding to 6.33 and 6.25 nm (−20 °C), respectively. The position of these two peaks show different temperature dependencies upon heating suggesting they originate from different structural features. The peak at 6.33 nm is assigned to a lamellar structure on the basis of a higher-order reflections of the repeat (data not shown) and the wide-angle data indicates the presence of gel phase which must be lamellar. The peak at 6.25 nm shows the same temperature dependency as the peak at 7.58 nm (−20 °C) that has been assigned to a ripple structure and is likely to be a reflection originating from the same structure.

To provide additional information on the structure of the ripple phase, electron micrographs of freeze-fracture replicas prepared from these dispersions thermally quenched from −10 °C were examined (Fig. 3c). These showed areas with a ripple structure consistent with an assignment of these additional peaks in the X-ray diffraction pattern as a ripple phase. The ripple phase seen in the freeze-fracture replicas has a periodicity of about 90 nm and is clearly different from the ripple phase formed by the pure phospholipid which has a ripple repeat of the (1,0) bands in the region of 17 nm (Fig. 1c). No (1,0) bands of a ripple phase, however, were observed in this mixture over the temperature range −21 to 9 °C, indicating that the presence of α-tocopherol prevented formation of ripple phase domains associated with the pure phospholipid.

A cooling scan of this mixture provided further evidence of the induction of a ripple phase by the presence of α-tocopherol (Fig. 3d,e). A broad first-order lamellar peak can be seen in the liquid–crystal phase at temperatures above 0 °C. The WAXS peak indicated transition to a lamellar gel phase with a mid-point temperature of about −5 °C. The lamellar spacing increased from about 6.7 to 7.5 nm during

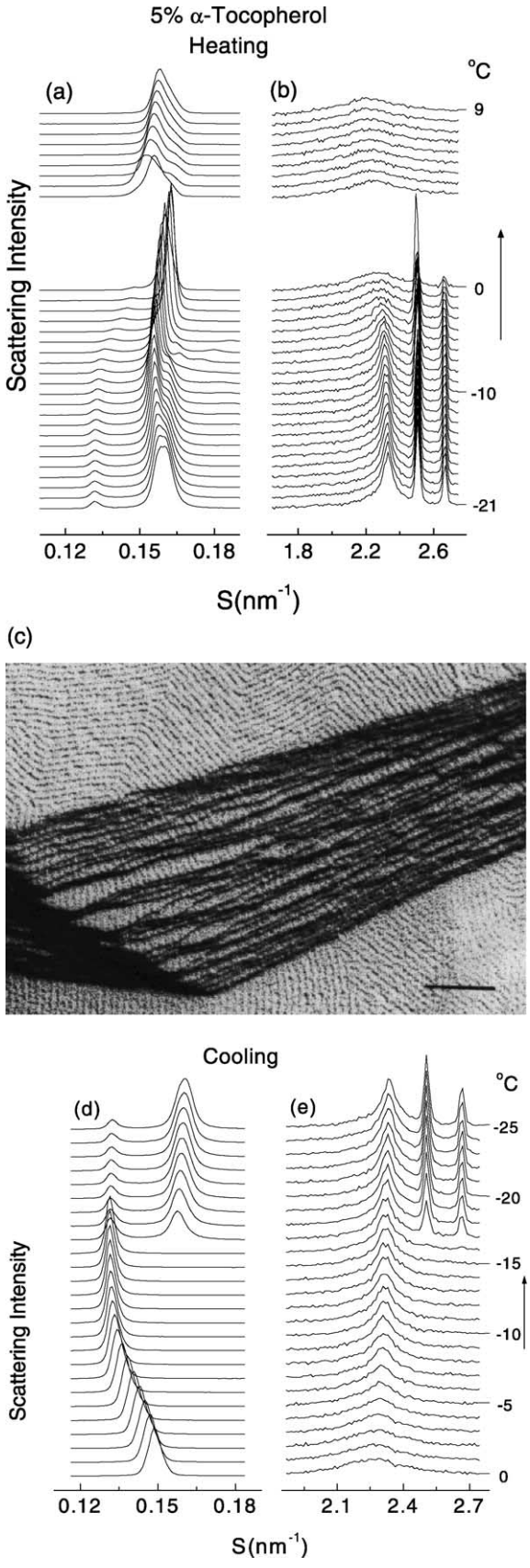

Fig. 3. Plots of scattering intensity profiles versus reciprocal spacing as a function of temperature of a codispersion of 5 mol% α-tocopherol in POPC recorded during a heating scan from −21 to 9 °C (a, SAXS; b, WAXS) and cooling from 0 to −25 °C (d, SAXS; e, WAXS) at 3°/min. Each diffraction pattern represents scattering accumulated in 10 seconds. (c). Electron micrograph of a freeze-fracture replica prepared from a codispersion of POPC containing 5 mol% α-tocopherol thermally quenched from −10 °C. The scale bar corresponds to 100 nm.

the gel to liquid–crystal phase transition. The dispersion remained in a supercooled state down to a temperature of −17 °C when peaks of hexagonal ice appeared. This was associated with an appearance of a new lamellar phase with a *d*-spacing of 6.2 nm and a corresponding decrease in the residual peak at 7.5 nm. This change in the diffraction pattern is consistent with a freeze-induced dehydration of the lamellar phase but no significant change in the superimposed ripple structure.

Increasing α-tocopherol to 10 mol% in POPC results in a change in the relative intensities of the diffraction maxima observed in the SAXS region. A sequence of scattering profiles recorded during heating from −24 to 6 °C is shown in Fig. 4a,b. Two repeat spacings of 7.8 and 6.3 nm (−20 °C) corresponding to the α-tocopherol-induced ripple phase and the lamellar repeat spacings, respectively, were detected. The main transition temperature, as judged by the change in intensity of the sharp WAXS peak at 0.43 nm and its replacement by a broad peak at 0.45 nm is at about −4 °C. Similar SAXS and WAXS intensity patterns were observed in a mixture of POPC containing 20 mol% α-tocopherol (Fig. 4c,d). The main transition temperature in this mixture is observed at about −6 °C. It is noteworthy that the ripple structure is preserved in the frozen dispersion despite transformation of the lamellar structure into a liquid–crystal phase and remnants of the ripple structure persist until reflections from hexagonal ice disappear. This suggests that the ripple structure is sustained by the freeze-induced dehydration and cannot relax into the smectic phase until rehydration occurs above 0 °C. The fluid phase of both these mixtures is characterised by two lamellar repeat spacings at about 6.4 and 6.1 nm, respectively. Based on the relative scattering intensities and the lamellar repeat spacing of pure POPC, the lamellar repeat at 6.4 nm could be assigned to an α-tocopherol-enriched lamellar phase separated from bilayers of pure phospholipid.

Phase assignments of the ripple structure induced by α-tocopherol are more clearly defined in plots of *d*-spacings of the SAXS peaks as a function of temperature shown in Fig. 5. The reflections arising from this ripple structure are different from those from the ripple phase formed by the pure phospholipid and the range of temperatures over which the induced ripple phase is observed is greatly extended. Of particular note is the temperature dependence of the two peaks seen in the mixture containing 5 mol% α-tocopherol which indicates they originate from the same structure which differs from that of the lamellar repeat. Previous freeze-fracture electron microscopic studies of the effect of α-tocopherol on the structure of saturated molecular species of phosphatidylcholines [19] reported that a disordered ripple structure of periodicity 50–150 nm is superimposed on a more regular ripple structure of periodicity 16–17 nm oriented perpendicular to the larger ripples in codispersions containing about 5 mol% α-tocopherol. The present results indicate that although the thermal characteristics of the α-tocopherol-induced ripple phase is similar in saturated and unsaturated molecular species of phosphatidylcholine the structure of the ripple phase is different. Moreover, the ripple structure is present

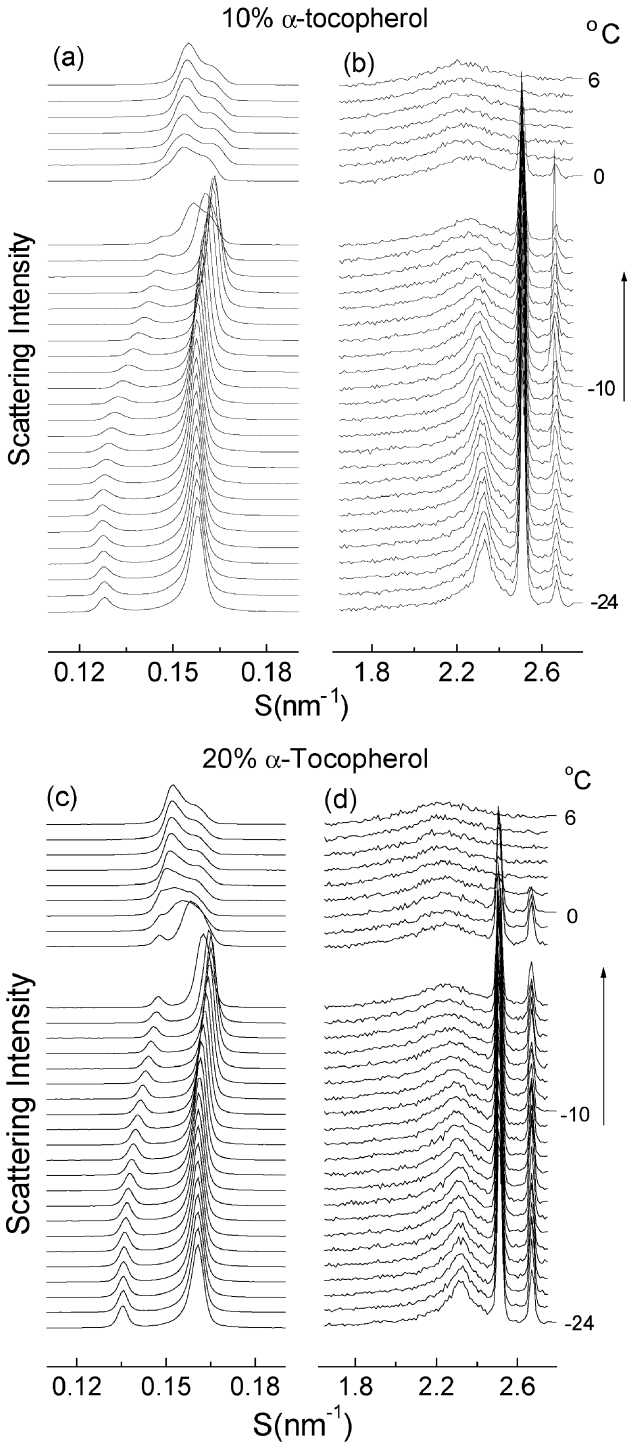

Fig. 4. Plots of scattering intensity profiles versus reciprocal spacing as a function of temperature of a codispersion of 10 mol% (a, SAXS; b, WAXS) and 20 mol% (c, SAXS; d, WAXS) α-tocopherol in POPC recorded during heating scans from −24 to 6 °C at 3°/min. Each diffraction pattern represents scattering accumulated in 10 s.

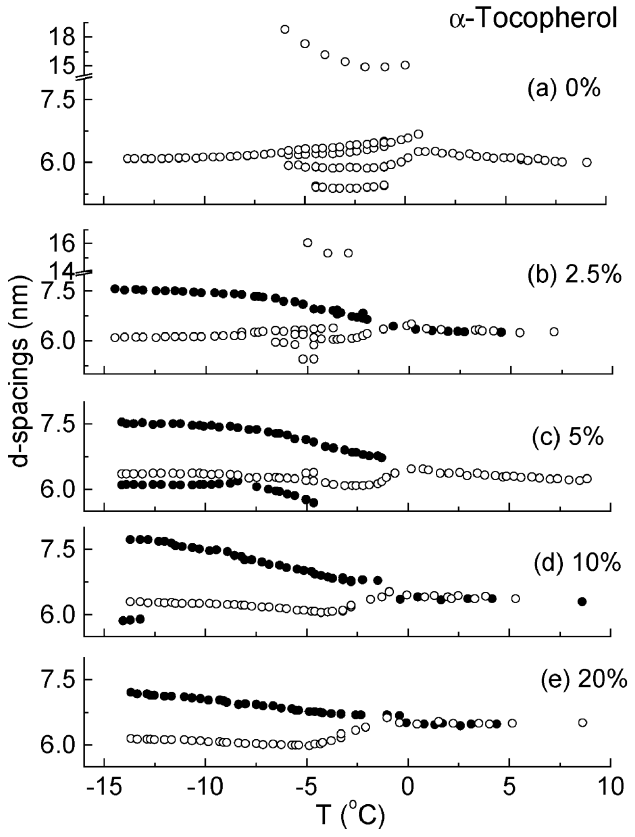

Fig. 5. Small-angle diffraction *d*-spacings versus temperature during heating of mixed aqueous dispersions of POPC containing (a) 0 mol%; (b) 2.5 mol%; (c) 5 mol%; (d) 10 mol%; and (e) 20 mol% α-tocopherol. The symbols (○) and (●) indicate, respectively, the pure phospholipid and the α-tocopherol-rich domains.

in dispersions containing up to 20 mol% α-tocopherol in POPC whereas in saturated phosphatidylcholines no ripple phases were induced in codispersions containing more than 10 mol% α-tocopherol.

This is illustrated in logarithmic plots of scattering intensity in the SAXS region of mixtures containing varying proportions of α-tocopherol in Fig. 6a. The peak associated with the ripple phase at a spacing of about 7.5 nm is seen in all mixed dispersions at both −5 and −15 °C. The effect of α-tocopherol on the hydrocarbon chain packing in the bilayers is shown in Fig. 6b in which the scattering intensity from the corresponding WAXS peaks are plotted. This shows that increasing amounts of α-tocopherol caused progressive disordering of the hydrocarbon chains in the temperature region below the gel to liquid–crystal phase transition of the pure phospholipid. A more detailed examination of the WAXS data was undertaken using plots of the WAXS intensity vs. temperature and a summary of the results is presented in Fig. 7. This shows that increasing amounts of α-tocopherol in dispersions of POPC cause a progressive reduction in the mid-point of the gel to liquid–crystal phase transition temperature and cooperativity of the transition as seen by an increase in the temperature range over which the transition take place. This is consistent with

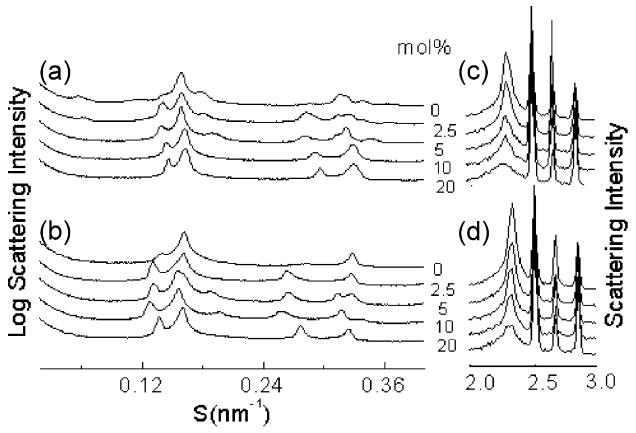

Fig. 6. A comparison of the X-ray diffraction profiles of codispersions of POPC with different amounts of α-tocopherol. Logarithm scattering intensity profiles in the SAXS region at (a) −5 °C and (b) −15 °C; corresponding WAXS intensity profiles at (c) −5 °C and (d) −15 °C.

the effect of α-tocopherol on enthalpy changes during the main transition of phosphatidylcholines recorded by calorimetry [17,18].

The present results are consistent with a model in which α-tocopherol molecules interpolate between POPC molecules in bilayer arrangement. At temperatures lower than the main gel to liquid–crystal phase transition temperature of POPC, a characteristic ripple phase is induced and this is stabilized by freeze-induced dehydration. Phase separation of bilayers of POPC enriched in α-tocopherol from domains of phospholipid depleted of α-tocopherol is observed in the fluid phase. This infers that α-tocopherol is not distributed randomly in the lipid matrix of biological membranes but may be phase separated in α-tocopherol-enriched domains.

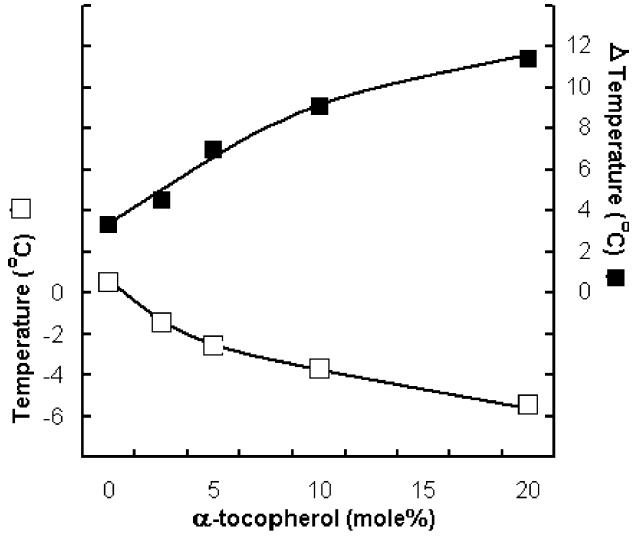

Fig. 7. Effect of α-tocopherol on the temperature of the main transition temperature (T_m). Normalized WAXS intensity profiles were calculated as a function of temperature. T_m (□) was determined as the temperature of half maximum intensity and the onset and completion temperatures defined the width of the transition (■).

How this distribution might relate to the function of α-tocopherol has yet to be determined.

Acknowledgements

Financial support and beam time for the experiments was obtained from the Daresbury Laboratory. X.W. is supported by a KC Wong Education Foundation Studentship. The assistance of Dr. Konrad Semmler for the freeze-fracture electron microscopy is gratefully acknowledged.

References

[1] M. Scarpa, A. Rigo, M. Maiorino, F. Ursini, C. Gregolin, Biochim. Biophys. Acta 801 (1984) 215–219.
[2] B. Halliwell, J.M.C. Gutteridge, Free Radicals in Biology and Medicine, Clarendon Press, Oxford, 1991.
[3] H. Sies, Oxidative Stress: Oxidants and Antioxidants, Academic Press, San Diego, 1991.
[4] D.C. Liebler, Crit. Rev. Toxicol. 23 (1993) 147–169.
[5] K. Fukuzawa, K. Matsuura, A. Tokumura, A. Suzuki, J. Terao, Free Radic. Biol. Med. 22 (1997) 923–930.
[6] V.E. Kagan, Ann. N. Y. Acad. Sci. 570 (1988) 120–135.
[7] V.E. Kagan, P.J. Quinn, Eur. J. Biochem. 171 (1988) 661–667.
[8] P.J. Quinn, Eur. J. Biochem. 233 (1995) 916–925.
[9] M. Sanchezmigallon, F.J. Aranda, J.C. Gomez-Fernandez, Biochim. Biophys. Acta 1279 (1996) 251–258.
[10] M. Sanchezmigallon, F.J. Aranda, J.C. Gomez-Fernandez, Biochim. Biophys. Acta 1281 (1996) 23–30.
[11] J. Salgado, J. Villalian, J.C. Gomez-Fernandez, Biochim. Biophys. Acta 1239 (1995) 213–225.
[12] V. Micol, F.J Aranda, J. Villalian, J.C. Gomez-Fernandez, Biochim. Biophys. Acta 1022 (1990) 194–202.
[13] T. Lefevre, M. Picquart, Biospectroscopy 2 (1996) 391–403.
[14] B. DeKruijff, P.W.M. Van Dijck, R.A. Demel, A. Schuijff, F. Brants, L.L.M. Van Deenen, Biochim. Biophys. Acta 356 (1974) 1–7.
[15] J.B. Massey, H.S. She, H.J. Pownall, Biochem. Biophys. Res. Commun. 106 (1982) 842–847.
[16] J. Villalain, F.J. Aranda, J.C. Gomez-Fernandez, Eur. J. Biochem. 158 (1986) 141–147.
[17] A. Ortiz, F.J. Aranda, J.C. Gomez-Fernandez, Biochim. Biophys. Acta 898 (1987) 214–222.
[18] E.J. McMurchie, G.H. McIntosh, J. Nutr. Sci. Vitaminol. 32 (1986) 551–558.
[19] X. Wang, K. Semmler, W. Richter, P.J. Quinn, Arch. Biochem. Biophys. 377 (2000) 304–314.
[20] X. Wang, P.J. Quinn, Biochim. Biophys. Acta 1509 (2000) 361–372.
[21] X. Wang, P.J. Quinn, Eur. J. Biochem. 267 (2000) 6362–6368.
[22] X. Wang, P.J. Quinn, Eur. J. Biochem. 264 (1999) 1–8.
[23] X. Wang, H. Takahashi, I. Hatta, P.J. Quinn, Biochim. Biophys. Acta 1418 (1999) 335–343.
[24] D.M. Small, Curr. Opin. Struct. Biol. 8 (1998) 413–416.
[25] B.A. Cunningham, W. Bras, P.J. Quinn, L.J. Lis, J. Biochem. Biophys. Methods 29 (1994) 87–111.
[26] C. Boulin, R. Kempf, M.H.J. Koch, S.M. McLauchlin, Nucl. Instrum. Methods Phys. Res., A 249 (1986) 399–407.
[27] A. Bigi, N. Roveri, Fibre diffraction: collagen, in: S. Ebashi, M. Koch, E. Rubenstein (Eds.), Handbook on Synchrotron Research, vol. 4, Elsevier, The Netherlands, 1991, pp. 25–37.
[28] E.J. Addink, J. Beintema, Polymer 2 (1961) 185–187.